

Integral transforms of the quantum mechanical path integral: Hit function and path-averaged potential

James P. Edwards,^{1,*} Urs Gerber,^{1,2,†} Christian Schubert,^{1,‡} Maria Anabel Trejo,^{1,3,§} and Axel Weber^{1,||}

¹*Instituto de Física y Matemáticas, Universidad Michoacana de San Nicolás de Hidalgo, Edificio C-3, Apdo. Postal 2-82, C.P. 58040, Morelia, Michoacán, Mexico*

²*Instituto de Ciencias Nucleares, Universidad Nacional Autónoma de México, A.P. 70-543, C.P. 04510 Ciudad de México, México*

³*Theoretisch-Physikalisches Institut, Friedrich-Schiller-Universität Jena, Max-Wien-Platz 1, 07743 Jena, Germany*



(Received 25 October 2017; published 10 April 2018)

We introduce two integral transforms of the quantum mechanical transition kernel that represent physical information about the path integral. These transforms can be interpreted as probability distributions on particle trajectories measuring respectively the relative contribution to the path integral from paths crossing a given spatial point (the *hit function*) and the likelihood of values of the line integral of the potential along a path in the ensemble (the *path-averaged potential*).

DOI: [10.1103/PhysRevE.97.042114](https://doi.org/10.1103/PhysRevE.97.042114)

I. INTRODUCTION

In the standard quantum mechanics of a particle in a time-independent potential $V(\mathbf{r})$, a fundamental quantity is the propagator, $K(y, x; T)$, defined as the matrix element of the evolution operator in configuration space:

$$K(y, x; T) = \langle y | e^{-iHT} | x \rangle, \quad (1)$$

with the Hamiltonian $H = \frac{p^2}{2m} + V(\mathbf{r})$ (using natural units). The propagator holds the complete information on the time evolution of the system, satisfying the Schrödinger equation, $i\partial_T K(y, x; T) = H(y)K(y, x; T)$ with $H(y) = -\frac{1}{2m}\partial_y^2 + V(y)$ satisfying boundary condition $\lim_{T \rightarrow 0} K(y, x; T) = \delta(x - y)$, so knowing its explicit form is tantamount to solving the system.

In a basis of eigenfunctions of H the propagator has spectral representation [henceforth working in Euclidean space-time so $K(T) = e^{-TH}$]

$$\sum_n \psi_n(y) \psi_n^*(x) e^{-E_n T} + \int dk \psi_k(y) \psi_k^*(x) e^{-E(k)T}, \quad (2)$$

where we have separated contributions from the bound states and the scattering states of the system.

The kernel for a scalar particle also has path-integral representation

$$K(y, x; T) = \int_{x(0)=x}^{x(T)=y} \mathcal{D}x e^{-\int_0^T dt [\frac{m\dot{x}^2}{2} + V(x(t))]}, \quad (3)$$

with the free path-integral normalization

$$K_0(y, x; T) = \int_{x(0)=x}^{x(T)=y} \mathcal{D}x e^{-\int_0^T dt \frac{m\dot{x}^2}{2}} = \left(\frac{m}{2\pi T}\right)^{\frac{D}{2}} e^{-\frac{m(y-x)^2}{2T}}. \quad (4)$$

The present paper introduces two representations of the propagator: the “hit function” $\overline{\mathcal{H}}(z|y, x; T)$ and the “path-averaged potential” $\overline{\mathcal{P}}(v|y, x; T)$. Both have the character of invertible integral transforms of the kernel,

$$K(y, x; T) = \int d^D z \overline{\mathcal{H}}(z|y, x; T), \quad (5)$$

$$K(y, x; T) = \int_{-\infty}^{\infty} dv \overline{\mathcal{P}}(v|y, x; T) e^{-v}. \quad (6)$$

Our original motivation for these representations lies in their usefulness for numerical sampling of the path integral (3): a good sampling of these distributions can help to mitigate the limitations of a direct sampling of the path integral, where often excessively large or small contributions to the propagator can be statistically unlikely and consequently undersampled; in cases where the approximate form of these distributions is known, a fit to their sampling can provide complementary information to that which is obtainable in traditional numerical calculations of the kernel function—see [1] for a related approach. We will report our corresponding results in a separate publication [2]; however, we anticipate that these representations will find much wider application, since they provide specific physical information on the dynamics of the system that would be unclear using standard techniques. The hit function has an analogy in the proper time formalism of quantum field theory (see [3,4]), whilst a relativistic analogy of the path-averaged potential has been introduced by Gies *et al.* [1]; here we adapt these objects for calculations in quantum mechanics and supply the inverse transformations lacking in [3] and [1]. We also explore their gauge dependency.

In the following we first define $\overline{\mathcal{P}}(v)$ and $\overline{\mathcal{H}}(z)$ and provide the inverse transformations to (5) and (6). We then discuss their

*Corresponding author: jedwards@ifm.umich.mx

†gerber@correo.nucleares.unam.mx

‡schubert@ifm.umich.mx

§mtrejo@ifm.umich.mx

||axel@ifm.umich.mx

asymptotic form for large T and their gauge transformations for electromagnetic interactions. Finally we calculate both functions for some simple potentials and show compatibility with numerical samplings.

II. TRANSFORMS OF THE KERNEL

In theoretical calculations and numerical simulations a direct determination of the kernel can be difficult, so it may be advantageous to consider some intermediate quantity. Here we present two such quantities.

A. Hit function, $\overline{\mathcal{H}}(z)$

The first quantity is a function of a spatial point, z , measuring the relative contribution to the propagator of paths which pass through z . This object, $\overline{\mathcal{H}}(z)$, which we call the ‘‘hit function’’ is defined by

$$\overline{\mathcal{H}}(z|y,x;T) \equiv \frac{1}{T} \int_{x(0)=x}^{x(T)=y} \mathcal{D}x \int_0^T \delta^D(z-x(\tau)) d\tau e^{-S[x]}, \quad (7)$$

where $S[x] = \int_0^T dt [\frac{m\dot{x}^2}{2} + V(x(t))]$ is the (Euclidean) classical action of the trajectory $x(t)$. The δ function counts the worldlines that cross through, or hit, the point z , weighting each path by its action. This function is inspired by a similar quantity called ‘‘local time’’ [5], measuring the time a fixed trajectory spends at a given point [6,7]. We have generalized this to include the weight associated to each trajectory and the external potential in computing its first moment. The path integral (7) is also similar to the contact interactions used in [8,9] and the field theory amplitudes developed in [3]. For later calculations it is convenient to introduce a properly normalized distribution on the space of trajectories

$$\mathcal{H}(z|y,x;T) \equiv \frac{\overline{\mathcal{H}}(z|y,x;T)}{K(y,x;T)}, \quad (8)$$

which integrates to unity.

Since $\overline{\mathcal{H}}(z)$ is built only out of particle worldlines that pass through the point z we can relate it to the kernel by forcing this criterion at some arbitrary time $0 < t < T$, leading to an inverse integral transform to (5),

$$\overline{\mathcal{H}}(z|y,x;T) = \frac{1}{T} \int_0^T dt K(z,x;t) K(y,z;T-t). \quad (9)$$

Note that the kernels in the integrand count *all* paths between the end points, including those that cross through z multiple times, in agreement with the δ function in (7). The Feynman Green function has been similarly decomposed in terms of restricted kernels in the ‘‘path decomposition expansion’’ of [10–12].

There are many approaches to numerical evaluation of the quantum mechanical path integral, such as Monte Carlo sampling [13–18] or, as we employ in [2], the adaptation of worldline numerics [19–22] to the nonrelativistic setting. In such cases, where the goal may be estimation of the kernel, knowledge of the hit function is sufficient, for one need simply integrate over positions in (7) or (9) to verify (5). So one could sample the hit function via its path-integral

representation (7) and determine the kernel through finite dimensional (numerical) integration.

B. Path-averaged potential, $\overline{\mathcal{P}}(v)$

The path-integral determination of the kernel amounts to the expectation value of exponentiated line integrals of the potential. This motivates describing the likelihood of values of these line integrals over particle paths with Gaussian distribution on their velocities. Denoting this function by $\overline{\mathcal{P}}(v)$ where $v \equiv \int_0^T V(x(t)) dt$ is the integral of the potential along the trajectory, $x(t)$, we express this likelihood as a constrained path integral:

$$\overline{\mathcal{P}}(v|y,x;T) \equiv \int_{x(0)=x}^{x(T)=y} \mathcal{D}x \delta\left(v - \int_0^T V(x(t)) dt\right) e^{-\int_0^T \frac{m\dot{x}^2}{2} dt}. \quad (10)$$

Prior use of a similar function has been made in relativistic quantum theory [1], where worldline numerics are used to sample the likelihood (a function of proper time) and functional fits are made to the numerical results.

Using the Fourier representation of the δ function we may write $\overline{\mathcal{P}}(v)$ in terms of the kernel,

$$\overline{\mathcal{P}}(v|y,x;T) = \frac{1}{2\pi} \int_{-\infty}^{\infty} dz e^{ivz} \tilde{K}(y,x;T,z), \quad (11)$$

where \tilde{K} is related to the kernel K by the substitution $V(x) \rightarrow izV(x)$ under the path integral. This follows if one may exchange the functional and Fourier integrations and gives the inverse transform to (6).

As before, we also introduce a normalized probability distribution by

$$\mathcal{P}(v|y,x;T) \equiv \frac{\overline{\mathcal{P}}(v|y,x;T)}{K_0(y,x;T)}, \quad (12)$$

which has unit area. Note in contrast to (8) the normalization for $\mathcal{P}(v)$ is always known analytically since it involves only the free kernel.

It is straightforward to check that (6) follows from (10) or (11), so numerical estimation of the kernel follows from the expectation of e^{-v} against the likelihood $\overline{\mathcal{P}}(v)$, again reducing the problem to a finite dimensional integral.

C. Asymptotic properties of the distribution functions

The spectral representation of the kernel (2) implies asymptotic formulas for our functions under suitable circumstances. This is useful when studying the large time $T \rightarrow \infty$ asymptotics of these distributions that are relevant when extracting the ground state energy, for example. We focus on the normalized distributions defined in (8) and (12).

For $\mathcal{H}(z)$ we substitute the spectral decomposition directly into (9). Subsequently integrating over the intermediate time t

leads to a double sum

$$\mathcal{H}(z|y,x;T) = \frac{1}{TK(y,x;T)} \left[T \sum_n \psi_n(y) |\psi_n(z)|^2 \psi_n^*(x) e^{-E_n T} + \sum_{n,m \neq n} \psi_n(y) \psi_n^*(z) \psi_m(z) \psi_m^*(x) \frac{e^{-E_n T} - e^{-E_m T}}{E_m - E_n} \right], \quad (13)$$

where we have only included contributions from bound states; indeed as $T \rightarrow \infty$, the leading contributions arise from states with least energy. Denoting the ground state energy (assumed nondegenerate) by E_0 we find the asymptotic form

$$\begin{aligned} \mathcal{H}(z|y,x;T) &\simeq |\psi_0(z)|^2 + \frac{1}{T\psi_0(y)\psi_0^*(x)} \\ &\times \sum_{n>0} \frac{\psi_0(y)\psi_0^*(z)\psi_n(z)\psi_n^*(x) + (n \leftrightarrow 0)}{E_n - E_0} \end{aligned} \quad (14)$$

up to contributions of order $e^{-(E_1-E_0)T}$. Note the leading order term on the right hand side has no dependence upon initial and final positions, as expected for late time evolution.

For $\mathcal{P}(v)$, the situation is more subtle, since sending $V(x) \rightarrow izV(x)$ modifies the Hamiltonian. Calculation of $\mathcal{P}(v)$ supposes the kernel can be analytically continued to a new kernel \tilde{K} . If the spectral decomposition can also be continued, with new ‘‘wave functions,’’ $\tilde{\psi}(x; z)$, and ‘‘energies,’’ $\tilde{E}_n(z)$ [we shall see that, for the harmonic oscillator with frequency ω , $E_n \rightarrow \tilde{E}_n(z) = \frac{1 \pm i}{\sqrt{2}} \omega \sqrt{|z|} (n + \frac{1}{2})$] whose real parts remain bounded, there will still exist an energy, \tilde{E}_0 , satisfying $\text{Re}(\tilde{E}_0) \leq \text{Re}(\tilde{E}_n)$ for $n > 0$. Then we get a large- T asymptotic formula

$$\tilde{K}(y,x;T) \simeq \sum_{n_0} \tilde{\psi}_{n_0}(y; z) \tilde{\psi}_{n_0}^*(x; z) e^{-\tilde{E}_{n_0}(z)T}, \quad (15)$$

where the sum is over states with $\text{Re}(\tilde{E}_{n_0}) = \text{Re}(\tilde{E}_0)$. Substituting this asymptotic representation into (11) we learn that, for large T ,

$$\begin{aligned} \mathcal{P}(v|y,x;T) &\simeq \frac{1}{2\pi K_0(y,x;T)} \\ &\times \sum_{n_0} \int_{-\infty}^{\infty} dz e^{ivz} \tilde{\psi}_{n_0}(y; z) \tilde{\psi}_{n_0}^*(x; z) e^{-\tilde{E}_{n_0}(z)T}, \end{aligned} \quad (16)$$

giving one approach to studying the asymptotics of $\mathcal{P}(v)$.

D. Electromagnetic interactions

For a particle coupled to a gauge potential, \mathcal{A} , we must also consider the inherent gauge freedom. The (Euclidean) action is

$$S[x, \mathcal{A}] = \int_0^T dt \left[\frac{m\dot{x}^2}{2} + ie\mathcal{A}(x(t)) \cdot \dot{x} \right]. \quad (17)$$

Given a reference gauge, with potential $\hat{\mathcal{A}}$, the kernel with respect to this gauge, $\hat{K}(y,x;T)$, changes covariantly under a gauge transformation $\hat{\mathcal{A}}_\mu(x) \rightarrow \mathcal{A}_\mu(x) = \hat{\mathcal{A}}_\mu(x) + \partial_\mu \Lambda(x)$ as [23]

$$K(y,x;T) = e^{-ie\varphi(y,x)} \hat{K}(y,x;T), \quad (18)$$

with $\varphi(y,x) \equiv \int_x^y (\mathcal{A} - \hat{\mathcal{A}}) dx = \Lambda(y) - \Lambda(x)$ the holonomy exponent for the difference between the gauge potentials. We will describe the implications for the distributions $\mathcal{H}(z)$ and $\mathcal{P}(v)$.

The distribution $\mathcal{H}(z)$ can be defined to be gauge invariant, although it now becomes complex valued. Using formula (9) with the kernels written in a specific gauge,

$$\hat{\mathcal{H}}(z|y,x;T) = \frac{1}{T\hat{K}(y,x;T)} \int_0^T dt \hat{K}(z,x;t) \hat{K}(y,z;T-t), \quad (19)$$

gauge transforming the kernels on the right hand side leads to the transformed hit function distribution

$$\mathcal{H}(z|y,x;T) = \frac{e^{-ie[\varphi(z,x)+\varphi(y,z)]}}{e^{-ie\varphi(y,x)}} \hat{\mathcal{H}}(z|y,x;T). \quad (20)$$

Here we have used the fact that the holonomy is independent of the path. The phase factors cancel so that $\mathcal{H}(z|y,x;T) = \hat{\mathcal{H}}(z|y,x;T)$ is invariant [$\hat{\mathcal{H}}(z)$ picks up a phase $-ie\varphi(y,x)$] and we may choose a convenient gauge for its computation.

We also modify our formula for $\mathcal{P}(v)$ to become a real-valued distribution on the phase introduced by the potential. This distribution will be gauge dependent, so we begin by defining $\hat{\mathcal{P}}(v|y,x;T)$ with respect to our reference gauge as

$$\begin{aligned} \frac{1}{K_0(y,x;T)} \int_{x(0)=x}^{x(T)=y} \mathcal{D}x \delta \left(v - e \int_0^T \hat{\mathcal{A}} \cdot \dot{x} d\tau \right) e^{-\int_0^T dt \frac{m\dot{x}^2}{2}} \\ = \frac{1}{2\pi K_0(y,x;T)} \int_{-\infty}^{\infty} dz e^{ivz} \tilde{K}(y,x;T,z), \end{aligned} \quad (21)$$

where now \tilde{K} requires scaling $e \rightarrow ze$. Under a gauge transformation to a general potential \mathcal{A} the distribution becomes

$$\frac{1}{2\pi K_0(y,x;T)} \int_{-\infty}^{\infty} dz e^{ivz - ie\varphi(y,x)z} \tilde{K}(y,x;T,z), \quad (22)$$

which is just $\hat{\mathcal{P}}(v - e\varphi(y,x)|y,x;T)$, so changing gauge translates the distribution by $e[\Lambda(y) - \Lambda(x)]$. For this reason, only the shape of the distribution is gauge invariant [the same holds for $\overline{\mathcal{P}}(v)$]. These gauge transformations follow also from the definitions (7) and (10).

III. APPLICATIONS

In this section we give explicit expressions for the distributions $\mathcal{H}(z)$ and $\mathcal{P}(v)$ for some simple potentials and compare our analytic results to sampling based upon worldline numerics. We cover quadratic potentials encompassing the free particle, linear potential, and the harmonic oscillator followed by a constant magnetic field, calculating the distributions using standard path-integral techniques. We present detailed results on numerical estimation of their kernels elsewhere [2].

A. Hit function

For $H(z)$, it is instructive to use the path-integral representation (7). For illustration, consider an action quadratic in the trajectory ($m = 1$ henceforth),

$$S[x] = \int_0^T dt \left[x \cdot \frac{1}{2} M \cdot x + b \cdot x \right], \quad (23)$$

whose classical solution satisfies $M \cdot x_c + b = 0$ with boundary conditions $x_c(0) = x$, $x_c(T) = y$. Expanding about this solution and invoking the Fourier representation of the δ function, Eqs. (8) and (7) yield

$$T\mathcal{H}(z|y,x;T) = \int_0^T d\tau \int \frac{d^D s}{(2\pi)^D} e^{is[z-x_c(\tau)] - \frac{s^2}{2} G_M(\tau,\tau)}, \quad (24)$$

where $G_M(\tau,\tau')$ is the “worldline” Green function [4,24] for M satisfying Dirichlet boundary conditions $G_M(0,\tau') = 0 = G_M(T,\tau')$. The Gaussian integral over s provides

$$\mathcal{H}(z|y,x;T) = \int_0^T \frac{d\tau}{T(2\pi G_M(\tau,\tau))^{\frac{D}{2}}} e^{-\frac{[z-x_c(\tau)]^2}{2G_M(\tau,\tau)}}, \quad (25)$$

which is suitable for numerical integration. For the free particle the worldline Green function for $M = -\frac{d^2}{dt^2}$ is $G_M(t,t') = -\Delta(t,t')$, where $\Delta(t,t') = \frac{1}{2}|t-t'| - \frac{1}{2}(t+t') + \frac{tt'}{T}$, and $x_c(t)$ is the straight line path from x to y , so that in one dimension the hit function is

$$\mathcal{H}_0(z|y,x;T) = \int_0^1 \frac{du}{\sqrt{2\pi Tu(1-u)}} e^{-\frac{[z-x-(y-x)u]^2}{2Tu(1-u)}}. \quad (26)$$

Here we have scaled $\tau = Tu$ and used $x_c(t) = x + (y-x)\frac{t}{T}$. This form can also be derived from (9), using (4), to verify the inversion formula. After suitable manipulation the integral can be written in terms of the complementary error function¹ as

$$\mathcal{H}_0(z|y,x;T) = \sqrt{\frac{\pi}{2T}} e^{\frac{(x-y)^2}{2T}} \operatorname{Erfc} \left[\frac{|z-x| + |z-y|}{\sqrt{2T}} \right], \quad (27)$$

¹We are indebted to Václav Zatloukal for drawing attention to aspects of local-time calculations which relate the free particle hit function to the error function. For this function we use the standard notation $\operatorname{Erfc}(\chi) \equiv 1 - \frac{2}{\sqrt{\pi}} \int_0^\chi e^{-\rho^2} d\rho$.

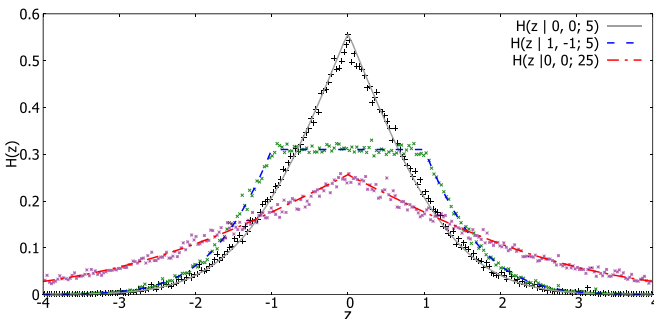


FIG. 1. $\mathcal{H}(z|y,x;T)$, for the free particle in one dimension. The solid line plots (27) and the data points represent a numerical sampling. Translating the initial and final point shifts the hit function due to translational symmetry.

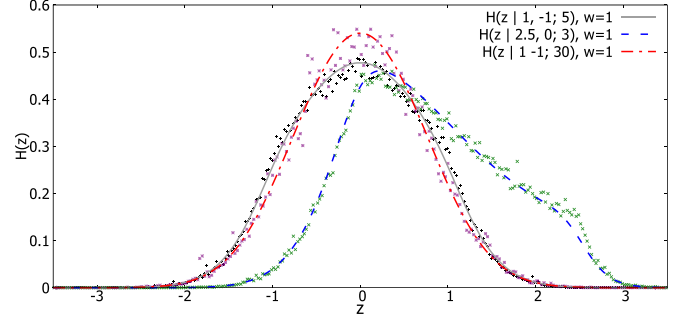


FIG. 2. $\mathcal{H}(z|y,x;T)$ for the harmonic oscillator in one dimension, $\omega = 1$. The solid line is a numerical evaluation of the hit function distribution and the data points represent a numerical sampling; increasing T , the distribution resembles $|\psi_0(z)|^2$ as in (14).

whose form is familiar in the context of Lévy random walks [7]. In Fig. 1 we show the distribution for suitable values of x , y , and T along with simulated samples based on worldline numerics.

For the one dimensional linear potential ($M = -\frac{d^2}{dt^2}$, $b = k$) the Green function is unchanged but the classical solution becomes $x_L(t) = x + (\frac{y-x}{T} - \frac{kT}{2})t + \frac{kt^2}{2}$ inducing the appropriate change in the exponent of (25), which must subsequently be integrated numerically. Worldline numerics are in excellent agreement with the result that ensues. For the harmonic oscillator, $M = -\frac{d^2}{dt^2} + \omega^2$, and we require the coincident Green function [25]

$$G_\omega(\tau,\tau) = \frac{1}{\omega} \frac{\sinh(\omega\tau) \sinh[\omega(T-\tau)]}{\sinh(\omega T)}. \quad (28)$$

We show the numerical evaluation of (25) for the harmonic oscillator and its correspondence with a sampling of the distribution using worldline numerics in Fig. 2. As for the free particle, one may verify the formulas via (9) using the well known kernels given in [26].

Note that for actions that are not quadratic and where it is not feasible to compute the path integral, formula (25) can be applied as a semiclassical approximation given sufficiently good knowledge of x_c .

Finally, we consider particle motion in a plane threaded by a perpendicular, constant magnetic field, B . A useful gauge is Fock-Schwinger gauge about the end point x , whereby $\hat{A}_\mu(x(t)) = -\frac{1}{2}F_{\mu\nu}(x(t) - x)^\nu$. This reduces the action to one that is quadratic in the trajectory [27] so that we may use (25) with $M = -\frac{d^2}{dt^2} \mathbb{1} + ieF \cdot \frac{d}{dt}$. The coupling to the gauge potential is absorbed into the worldline Green function, $\mathcal{G}_{\mu\nu}(t,t')$ given in Appendix B. To achieve this, one expands about the straight line path, denoted by $x_0(t)$, so that

$$\mathcal{H}(z|y,x;T) = \int_0^T \frac{dt}{2\pi T} \frac{e^{-\frac{1}{2}[z-x(t)]^\top \cdot \mathcal{G}^{-1}(t,t) \cdot [z-x(t)]}}{\det[\mathcal{G}(t,t)]}, \quad (29)$$

where $x(t) = x_0(t) - \frac{e}{T} \int_0^T \mathcal{G}(t,t') dt' \cdot (y-x)$.

B. Path-averaged potential

Turning to the path-averaged potential, it is easy to see from (10) that for a free particle $\mathcal{P}(v) = \delta(v)$. For the linear potential,

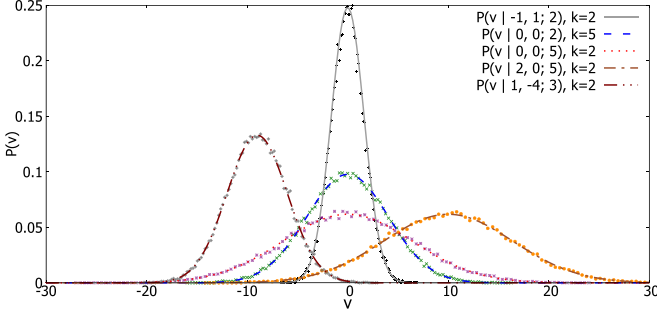


FIG. 3. $\mathcal{P}(v)$ for the linear potential $V(x) = kx$ for various parameters x , y , T , and k in one dimension. The points represent a computational sampling of the distribution using worldline numerics; lines are theoretical fits based upon (31).

$V(x) = kx$, the kernel $K(y, x; T)$ is [26]

$$K(y, x; T) = \sqrt{\frac{1}{2\pi T}} e^{[-\frac{1}{2T}(x-y)^2 - \frac{kT}{2}(x+y) + \frac{k^2 T^3}{24}]}, \quad (30)$$

and to effect the change $V \rightarrow izV$ it suffices to send $k \rightarrow izk$. Application of (11) supplies

$$\mathcal{P}(v|y, x; T) = \sqrt{\frac{6}{\pi k^2 T^3}} e^{-\frac{3}{2T}(x+y)^2} e^{-\frac{6}{k^2 T^3}[v^2 - kT(x+y)v]}, \quad (31)$$

which is a function of the sum of the end points. In Fig. 3 we demonstrate the analytic result and its agreement with numerical sampling. The limit $k \rightarrow 0$ supplies the δ function distribution of the free particle and one may verify (6) from (31) directly.

For the harmonic oscillator, Eq. (11) leads to a highly oscillatory z integral that must be evaluated numerically. Since the spectrum consists only of bound states, it is advantageous to apply instead the scaling $\omega \rightarrow \sqrt{iz}\omega$ directly in the spectral decomposition (2) and to take the real part of the integral over z along the positive real line. Then the energies scale to $\tilde{E}_n = \frac{1+i}{2}\sqrt{z}E_n$ whose real parts maintain their original ordering. This leads to a sum of Fourier integrals

$$\begin{aligned} & \pi K_0(y, x; T) \mathcal{P}(v|y, x; T) \\ &= \sqrt{\frac{\omega}{\pi}} \sum_{n \geq 0} \frac{1}{2^n n!} \text{Re} \int_0^\infty dz (iz)^{\frac{1}{4}} e^{ivz} e^{-\frac{1}{2}(\tilde{x}^2 + \tilde{y}^2) - \sqrt{iz}\omega T(n + \frac{1}{2})} \\ & \quad \times H_n(\tilde{x}) H_n(\tilde{y}) \end{aligned} \quad (32)$$

for $\tilde{x}^2 \equiv \sqrt{iz}\omega x^2$ and $\tilde{y}^2 \equiv \sqrt{iz}\omega y^2$. To make analytic headway, we set $x = 0 = y$, so that only states with n even contribute; the z integral can now be written in terms of modified Bessel functions of the second kind, K_n . The resulting sum (set $v_n = \frac{[(n + \frac{1}{2})\omega T]^2}{8v}$ for brevity),

$$\begin{aligned} \mathcal{P}(v|0, 0; T) &= 64\Theta(v) \sqrt{\frac{\omega T}{2\pi^2}} \sum_{n \text{ even}} \frac{n! v_n^{\frac{3}{2}} e^{-v_n}}{2^{n + \frac{1}{2}} (\frac{n}{2})!^2 [(n + \frac{1}{2})\omega T]^{\frac{5}{2}}} \\ & \quad \times \text{Re} \left[\left(v_n - \frac{3}{4} \right) K_{-\frac{1}{4}}(-v_n) - v_n K_{-\frac{5}{4}}(-v_n) \right], \end{aligned} \quad (33)$$

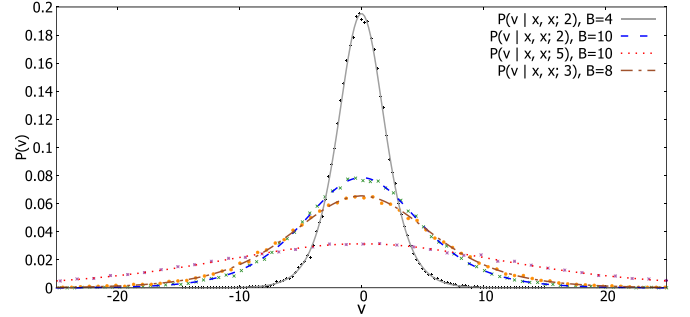


FIG. 4. $\hat{\mathcal{P}}(v)$ for a constant magnetic field ($e = 1$ and in Fock-Schwinger gauge) and $x = y$ for illustrative values of T and B . Lines are analytic curves using (36) overlaid on a sampling of the distribution from a worldline numerics simulation.

converges extremely rapidly so is apt for truncation to arbitrary accuracy [$\Theta(v)$ is the Heaviside step function indicating that $v \geq 0$]. We have checked this gives excellent agreement with sampled data generated by worldline numerics (truncation to $n \leq 30$ is more than sufficient) which will be presented in [2].

Finally we return to the case of a constant magnetic field. We continue to use the Fock-Schwinger gauge, since (22) allows simple transformation to other gauges. The reference kernel evaluates to [26]

$$\hat{K}(y, x; T) = \frac{eB}{4\pi \sinh(\frac{eBT}{2})} e^{-\frac{eB}{4}|x-y|^2 \coth(\frac{eBT}{2})}. \quad (34)$$

Sending $e \rightarrow ze$ and using (21) we must evaluate

$$\frac{eBT}{4\pi} \int_{-\infty}^{\infty} dz \frac{z}{\sinh(\frac{eBTz}{2})} e^{ivz - \frac{eBz}{4}|x-y|^2 \coth(\frac{eBTz}{2})}. \quad (35)$$

For arbitrary x and y this is easily evaluated numerically but we can make analytic progress for the diagonal elements, which by translational symmetry are all equal. In this case the z integral can be computed by closing the contour in the upper half plane, leading to

$$\hat{\mathcal{P}}(v|x, x; T) = \frac{\pi}{2eBT} \text{sech}^2\left(\frac{\pi v}{eBT}\right). \quad (36)$$

This result bears close similarity to the distributions used in numerical evaluation of the Euler-Heisenberg effective action in a relativistic setting in [28]. See Fig. 4 for an illustration of the distribution and the close match provided by worldline numerics. Note that by taking $B \rightarrow 0$ we acquire a representation of the δ function as expected and that (6) holds (after changing $e^{-v} \rightarrow e^{-iv}$).

IV. CONCLUSION

We have introduced two integral transforms of the quantum mechanical kernel as tools to study the path integral. These functions contain statistical information about contributions to the path integral of different trajectories. In both cases we have given asymptotic formulas and discussed their behavior under gauge transformations, before demonstrating the distributions with some examples. These calculations are verified by numerical sampling based upon worldline numerics. Elsewhere we shall provide more detailed calculations and application to

more complex systems as an alternative approach to traditional kernel-based methods in quantum mechanics.

An outstanding issue remains the general validity of the complex continuation of the spectral decomposition of the kernel to determine $\bar{\mathcal{P}}(v)$. Although we did not rely solely upon this continuation, we recognize that this requires greater scrutiny (as discussed, for example, in [29,30]). We also aim to incorporate spin degrees of freedom into these calculations in future work by building upon existing worldline techniques for doing so.

ACKNOWLEDGMENTS

J.P.E. and C.S. wish to thank Petr Jizba and Václav Zatloukal for insightful discussions and for sharing their expertise on local time; their thanks also to the organizers of the Path Integration in Complex Dynamical Systems 2017 workshop and the warm hospitality of the Leiden Center. M.A.T. thanks Holger Gies and the TPI, Jena, for hospitality and support during the development of the computer code for worldline numerics employed in this analysis. C.S. would like to thank Erhard Seiler for useful discussions and correspondence. J.P.E. appreciates Íñigo L. Egusquiza making thoughtful comments and pointing out useful literature related to the hit function. J.P.E. and C.S. gratefully acknowledge funding from CONACYT through grant Ciencias Basicas 2014 No. 242461 and U.G. and A.W. acknowledge funding by Conacyt Project No. CB-2013/222812. A.W. is also grateful to CIC-UMSNH for support.

APPENDIX A: WORLDLINE NUMERICS

Worldline numerics, developed in [20–22] following preliminary investigation in [19], means a computational estimation of the path integral, which we have recently adapted to the nonrelativistic setting. The integral over trajectories is discretized to an ensemble average over a finite number, N_L , of paths, $\{x_n\}_{n=1}^{N_L}$, generated such that the distribution on their velocities corresponds to the kinetic term in the particle action. There are several algorithms for producing these trajectories [1,22] and in this work we used an optimized algorithm which we term LSOL, further details of which can be found in [2,31]. The line integral of the potential along these paths is then computed numerically by splitting it into N_p segments (this corresponds to a time discretization, maintaining continuous spatial coordinates) so that

$$\int_{x(0)=x}^{x(T)=y} \mathcal{D}x e^{-\int_0^T dt [\frac{1}{2}\dot{x}^2 + V(x(t))]} \rightarrow \frac{K_0(y,x;T)}{N_L} \sum_{n=1}^{N_L} e^{-\frac{T}{N_p} \sum_{i=1}^{N_p} V(x_n(\frac{i}{N_p}))}. \quad (\text{A1})$$

It is useful to absorb the boundary conditions of the path integral into a background field by expanding $x(t) = x_0(t) + q(t)$, where $x_0(t) = x + (y-x)\frac{t}{T}$ is the straight line path from x to y . Making a further scaling $t \rightarrow Tu$ and a field redefinition $q(t) \rightarrow \sqrt{T}q(t) = \sqrt{T}q(Tu)$ we may write the path integral as

$$K_0(y,x;T) \langle e^{-T \int_0^1 [V(x_0(Tu)) + \sqrt{T}q(Tu)] du} \rangle, \quad (\text{A2})$$

where the boundary conditions are now Dirichlet on the quantum fluctuations: $q(0) = 0 = q(1)$. For the ensemble average N_L is chosen sufficiently large that a good sampling of the space of trajectories results.

The hit function is sampled in one spatial dimension by implementing the δ function by recognizing the change of sign of $z - x_n$ and rewriting

$$\int \delta(z - x(\tau)) d\tau = \int \sum_{\tau_i: x(\tau_i)=z} \frac{\delta(\tau - \tau_i)}{|\dot{x}(\tau_i)|} d\tau, \quad (\text{A3})$$

where the τ_i are the times at which the trajectory intersects the point z . The derivative in the denominator is calculated numerically using a third order backward discretization. We used 150 000 loops and 10 000 points per loop to ensure a good sampling and estimation of discrete derivative. The path-averaged potential is sampled by calculating the value of $\int d\tau V(x(\tau))$ along each worldline, weighting these values by the exponential of the kinetic part of the particle action. In this case, 50 000 loops were used with 5000 points per loop. The values are then binned to form a histogram and we interpolate between the densities to form a smooth curve.

APPENDIX B: WORLDLINE GREEN FUNCTION FOR CONSTANT MAGNETIC BACKGROUND

The worldline Green function for a particle in a plane with a constant, perpendicular magnetic background field, B , satisfying Dirichlet boundary conditions is [32]

$$\mathcal{G}_{\mu\nu}(t,t') = -\frac{2}{B} \left[\delta_{\mu\nu} \cosh\left(\frac{Bt_-}{2}\right) - i\epsilon_{\mu\nu} \sinh\left(\frac{Bt_-}{2}\right) \right] \times \left[\Theta(t_-) \sinh\left(\frac{Bt_-}{2}\right) - \frac{\sinh\left(\frac{Bt}{2}\right) \sinh\left(\frac{B}{2}(T-t')\right)}{\sinh\left(\frac{BT}{2}\right)} \right], \quad (\text{B1})$$

where $t_- \equiv t - t'$, $\epsilon_{12} = 1 = -\epsilon_{21}$, and Θ is the Heaviside step function. One may check that $-\frac{d^2\mathcal{G}}{dt^2} + ieF \cdot \frac{d\mathcal{G}}{dt} = \delta(t - t')$. If the particle is also free to move perpendicular to the plane, then the Green function associated to that direction would be $-\Delta(t,t')$ as appropriate for a free particle discussed in the main text.

- [1] H. Gies, J. Sanchez-Guillen, and R. A. Vazquez, *J. High Energy Phys.* **08** (2005) 067.
 [2] J. P. Edwards, U. Gerber, C. Schubert, M. A. Trejo, and A. Weber (unpublished).

- [3] A. M. Polyakov, *Gauge Fields and Strings* (Harwood Academic Publishers, New York, 1987).
 [4] C. Schubert, *Phys. Rep.* **355**, 73 (2001).
 [5] P. Lévy, *Comp. Math.* **7**, 283 (1939).

- [6] P. Jizba and V. Zatloukal, *Phys. Rev. E* **92**, 062137 (2015).
- [7] V. Zatloukal, *Phys. Rev. E* **95**, 052136 (2017).
- [8] J. P. Edwards, *J. High Energy Phys.* **01** (2016) 033.
- [9] J. P. Edwards and P. Mansfield, *J. High Energy Phys.* **01** (2015) 127.
- [10] A. Auerbach and S. Kivelson, *Nucl. Phys. B* **257**, 799 (1985).
- [11] A. Auerbach, S. Kivelson, and D. Nicole, *Phys. Rev. Lett.* **53**, 411 (1984).
- [12] A. Auerbach, S. Kivelson, and D. Nicole, *Phys. Rev. Lett.* **53**, 2275 (1984).
- [13] A. Korzeniowski, J. L. Fry, D. E. Orr, and N. G. Fazleev, *Phys. Rev. Lett.* **69**, 893 (1992).
- [14] K. Binder, *Rep. Prog. Phys.* **60**, 487 (1997).
- [15] J. Rejcek, S. Datta, N. Fazleev, J. Fry, and A. Korzeniowski, *Comput. Phys. Commun.* **105**, 108 (1997).
- [16] B. J. Berne and D. Thirumalai, *Annu. Rev. Phys. Chem.* **37**, 401 (1986).
- [17] N. Makri, *J. Math. Phys.* **36**, 2430 (1995).
- [18] K. Carlsson, M. Gren, G. Bohlin, P. Holmvall, P. Sätterskog, and O. Ahlén, Master's thesis, Department of Fundamental Physics, Subatomic Physics, Chalmers University of Technology, Göteborg, 2011, p. 115.
- [19] T. Nieuwenhuis and J. A. Tjon, *Phys. Rev. Lett.* **77**, 814 (1996).
- [20] H. Gies and K. Langfeld, *Nucl. Phys. B* **613**, 353 (2001).
- [21] H. Gies and K. Langfeld, *Int. J. Mod. Phys. A* **17**, 966 (2002).
- [22] H. Gies, K. Langfeld, and L. Moyaerts, *J. High Energy Phys.* **06** (2003) 018.
- [23] W. Dittrich and H. Gies, in *Probing the Quantum Vacuum: Perturbative Effective Action Approach in Quantum Electrodynamics and Its Application*, Springer Tracts in Modern Physics Vol. 166 (Springer, Berlin, 2000), p. 1.
- [24] D. Fliegner, P. Haberl, M. G. Schmidt, and C. Schubert, *Ann. Phys. (N.Y.)* **264**, 51 (1998).
- [25] H. Kleinert, *Path Integrals in Quantum Mechanics, Statistics, Polymer Physics, and Financial Markets* (World Scientific, Singapore, 2004).
- [26] C. Grosche and F. Steiner, *Handbook of Feynman Path Integrals*, Springer Tracts in Modern Physics (Springer, Berlin, 1998).
- [27] A. Ahmad, N. Ahmadiaz, O. Corradini, S. P. Kim, and C. Schubert, *Nucl. Phys. B* **919**, 9 (2017).
- [28] H. Gies and K. Klingmüller, *Phys. Rev. D* **72**, 065001 (2005).
- [29] E. B. Davies, *Proc.: Math., Phys. Eng. Sci.* **455**, 585 (1999).
- [30] E. B. Davies and A. B. J. Kuijlaars, *J. London Math. Soc.* **70**, 420 (2004).
- [31] M. A. Trejo, Ph.D. thesis, Instituto de Física y Matemáticas, Universidad Michoacana de San Nicolás de Hidalgo, 2017, *Estados ligados en el formalismo línea de mundo*.
- [32] D. G. C. McKeon and T. N. Sherry, *Mod. Phys. Lett. A* **09**, 2167 (1994).